Finding the Specific Heat Capacity of Beryllium

Nikita Sichov - nsichov@ethz.ch
Supervisor: Li Botao - libota@student.ethz.ch

December 11, 2025

Contents

Abstract

The primary goal of our experiment is to find the volume-constant specific heat capacity of Beryllium over the range between about 140 K and 370 K. The specific heat capacity tells us how much energy is needed per mass of a material in order to increase the internal heat (temperature) of the material. We do this using a calorimeter, engineered to give precise readings of the temperature over a large range. Despite this we see that our final calculations tend to be very sporadic towards the higher temperature zone of our data leading to questioning of the eligibility of the experimental setup.

Introduction

Theoretical background of Heat Capacity

By definition, a heat capacity quantifies how much heat must be exerted on an object in order to increase its temperature:

$$C = \frac{\delta Q}{\delta T}$$

It's units are thereby $\frac{J}{K}$. There are two kinds of heat capacity, one heat capacity is defined over constant temperature and the over constant volume, throughout this experiment we will be interested in the latter calculation, but we will need the constant pressure variant due to the structure of our experiment.[2]

Dulong-Petit Law

The equipartition theorem states that at thermal equilibrium, energy is shared at equal amount between all quadratic terms.[3] With this the expected energy of any harmonic oscillator is given as:

$$U = \langle E \rangle = \frac{1}{2} f k_B T$$

where k_B is the Boltzmann constant and f is the number of degrees of freedom (quadratic terms). For the mole of a lattice atomical structure we thereby have:

$$C_V = \left(\frac{\partial U}{\partial T} \right)_V = 3 N_A k_B$$

This states that the heat capacity isn't temperature dependent, which we know to be experimentally untrue.

Einstein's Approach

In attempt to fix this, Einstein used quantum mechanics, where we assume the harmonic oscillators to be quantum and thereby have energies $E_n = (n + \frac{1}{2})\hbar\omega$ with $n = 0, 1, 2, ...$. Thereby we find the Boltzmann mean value of the energy as:

$$\langle E \rangle = \frac{1}{2}\hbar\omega + \frac{\sum_{n=0}^{\infty} n\hbar\omega e^{\frac{n\hbar\omega}{k_B T}}}{\sum_{n=0}^{\infty} e^{\frac{n\hbar\omega}{k_B T}}} = \frac{1}{2}\hbar\omega + \frac{\hbar\omega}{e^{\frac{\hbar\omega}{k_B T}} - 1}$$

Thereby giving the heat capacity:

$$C_V = 3 N_A k_B \frac{e^{\frac{\hbar\omega}{k_B T}}}{\left(e^{\frac{\hbar\omega}{k_B T}} - 1 \right)^2} \left(\frac{\hbar\omega}{k_B T} \right)^2 = 3 N_A k_B \frac{e^{\frac{\Theta_E}{T}}}{\left(e^{\frac{\Theta_E}{T}} - 1 \right)^2} \left(\frac{\Theta_E}{T} \right)^2$$

Where $\Theta_E := \frac{\hbar\omega_E}{k_B}$. This theory has a good qualitative depiction of heat capacity since the limits match experimentally, otherwise it struggles in all other quantitative aspects.

Einstein's theory clearly misses two important considerations, namely that all oscillators are independent of each other and that they oscillate at the same frequency. If we want to consider these aspects, we consider a spectral frequency distribution interpretation of Einstein's model:

$$U = 3 N_A \langle E(\omega_E, T) \rangle = 3 N_A \int_0^\infty \langle E(\omega, T) \rangle \delta(\omega - \omega_E) d\omega = \int_0^\infty \langle E(\omega, T) \rangle z(\omega) d\omega$$

Where $z(\omega)d\omega = 3 N_A \cdot \delta(\omega - \omega_E)d\omega$ for Einstein's single frequency distribution.

Debye's Theory

Going back to the idea of lattice structure, with a wavelength significantly larger than the lattice distance, we have elastic waves with a wavelength independent speed.

We consider the number of modes n with wavelengths larger than a given $\lambda_{\min}$ in a 3-dimensional lattice:

$$n = \frac{3}{8}\frac{4\pi}{3}\frac{V}{\pi^2 c^3}\omega^3$$

Where c is the speed of sound and V is the molar volume. We find the spectral frequency distribution using $z(\omega) = \frac{\partial n}{\partial \omega}$ as:

$$z(\omega)d\omega = \frac{\partial n}{\partial \omega} = \frac{V}{2\pi^2}\frac{3}{c^3}\omega^2 d\omega$$

where $\bar{c} = \left(\frac{3}{\frac{1}{c_l^3}+\frac{2}{c_{tr}^3}}\right)^{\frac{1}{3}}$ is the general speed of sound that considers the two transverse c_{tr} and one longitudinal waves c_l. Since we've only considered low frequency (large wavelength), we must also consider higher frequencies for the complete spectrum. We must therefore also take the range $[0, \omega_D]$ to fit the total number of modes, this is:

$$\int_0^{\omega_D} z(\omega)d\omega = \frac{V}{2}\frac{\omega_D^3}{\pi^2 \bar{c}^3} = 3N_A \Rightarrow \omega_D = \left(6N_A\pi^2\bar{c}^3 \cdot \frac{1}{V}\right)^{\frac{1}{3}}$$

So by Debye:

$$z(\omega) = \begin{cases} \frac{3V}{2\pi^2\bar{c}^3}\omega^2 = 3N_A \cdot \frac{3\omega^2}{\omega_D^3} & \text{for } 0 \leq \omega \leq \omega_D \\ 0 \end{cases}$$

Therefore:

$$U = \int_0^{\omega_D}\left(\frac{\hbar\omega}{2} + \frac{\hbar\omega}{e^{\frac{\hbar\omega}{k_B T}}-1}\right) \cdot 3N_A\frac{3\omega^2}{\omega_D^3}d\omega$$

from which we get the molar heat capacity as:

$$C_V\left(\frac{\theta}{T}\right) = 3R \cdot 3\left(\frac{T}{\theta}\right)^3 \int_0^{\frac{\theta}{T}} \frac{x^4 e^x}{(e^x-1)^2}dx = 3R \cdot D\left(\frac{\theta}{T}\right) \tag{1}$$

Where we summarize the integral and some coefficients within the Debye function $D\left(\frac{\theta}{T}\right)$.

Born's Approach

We further complicate our model by taking the mean speed of sound to be split into transversal and longitudinal waves, requiring both modes have a common minimal wavelength. From this we get:

$$\lambda_{min} = 2\pi\frac{c_l}{\omega_{D,l}} = 2\pi\frac{c_{tr}}{\omega_{D,tr}}$$

giving us:

$$z(\omega) = N_A \cdot \frac{3\omega^2}{\omega_{D,l}^3} + 2N_A \cdot \frac{3\omega^2}{\omega_{D,tr}^3}$$

Therefore:

$$C_{V,Born} = R\left(D\left(\frac{\theta_1}{T}\right) + 2D\left(\frac{\theta_{tr}}{T}\right)\right) \quad \text{where} \quad \theta_l = \frac{\hbar\omega_{D,l}}{k_B}; \theta_{tr} = \frac{\hbar\omega_{D,tr}}{k_B}$$

Unfortunately, this approach, although more theoretical aligned, isn't (in most cases) more precise than Debye's model. The spectral distribution is practically identical up to the interval, $[\omega_{D,tr}, \omega_D]$ which has a small difference in the resulting integral over all relevant frequencies, as seen in 1.
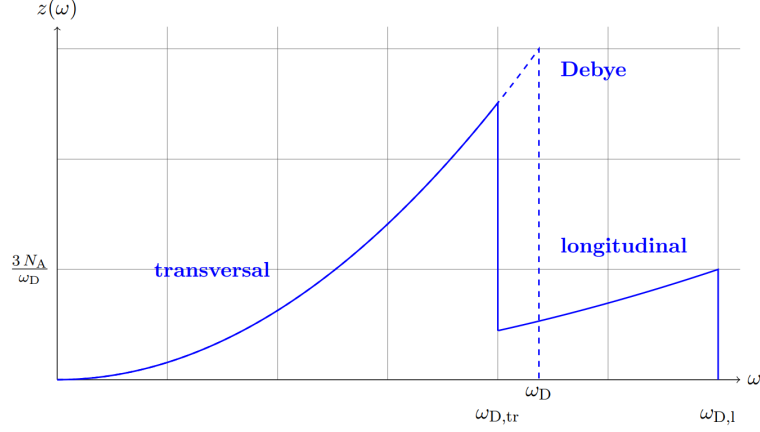
Figure 1: Frequency spectrum comparison of Debye's and Born's models

Heat capacity due to free electrons

For all the models we've entertained so far, we've approximated atomic lattice structure as individual harmonic oscillators. There remains the question of free electrons, which supposedly don't interact with these oscillators, but should nonetheless contribute to the structure of the solid. A key assumption is that these free electrons, lacking influence from potentials, can also be seen as a gas. This lets us use kinetic gas theory and claim that each free electron contributes $u_e = \frac{3}{2}k_B T$ to the internal energy of the solid. Thereby, the contribution to the heat capacity is $\frac{3}{2}k_B$.[1]. Therefore, we assume the total heat capacity of the metal to be:

$$C_V = C_{V \text{ (lattice)}} + C_{V \text{ (free electrons)}} = 3R + \frac{3R}{2} = \frac{9R}{2}$$

But this is flawed because, Dulong-Petit's law expects the heat capacity to be $3R$ at high temperature, the free electron must vanish in this limit. Assuming the electron to be an ideal gas creates degeneracy of the spin interaction of electrons, we must therefore turn to Fermi statistics. We get the result that due to the linearity of free electron heat capacity and the T^3 growth of the lattice heat capacity, we can neglect the electron term for temperatures larger than 15.9K where the two heat capacity contributions intersect as seen in Figure 2.

---

[1]The contribution of $\frac{3}{2}k_B$ is for each electron, an additional assumption is made that there is an equal amount of atoms as there are free electrons
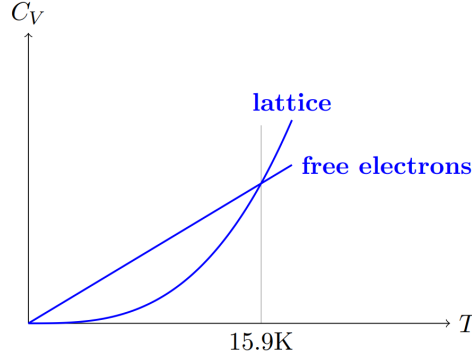
Figure 2: Heat capacity comparison of the lattice and free electron contribution

Experiment

We want to find the heat capacity of beryllium over the largest possible range of temperatures, for this experiment we take the range [-180,100]. For this we use the Nernst calorimeter, the diagram of which is found in Figure 3.
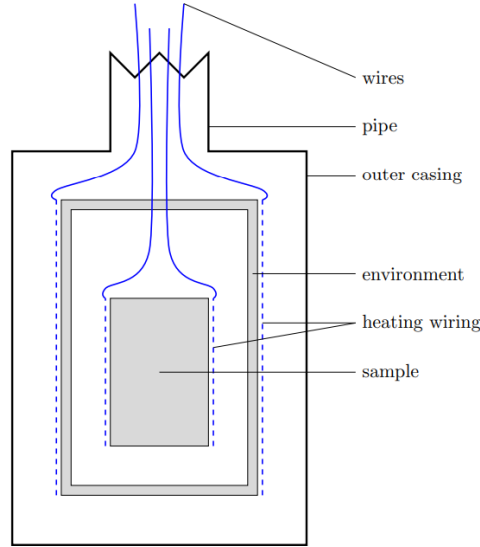

Figure 3: Diagram of the calorimeter

For the lower range we use liquid nitrogen. For this we take the exchange gas helium, which can heat the sample through the environment. When measuring, we isolate the sample by creating a vacuum that replace the exchange gas. Assuming the thermal conductance by other sources to be minimum. In addition to the heating done to the sample, we try to change the temperature of the environment to keep up with the sample thereby creating a layer of isolation from the fixed temperature of the exterior of the calorimeter. This minimizes heat radiation. Additionally, the temperature of the sample and environment are measured as differences to another element (in this case ice) that remains constant throughout the experiment.

5

Measurements

For the measurement of the experiment we consider an energy input and an energy effect. The input is the electric energy we feed into the system $A_{el} = VI \cdot t_h$ where V is the heating voltage V, I the heating the current and t_h is the heating time. The effect on the sample is the source of our heat capacity: $A_{th} = m \cdot c_p \cdot \Delta T$.

If we neglect all heat losses the energy input and effect are equal. But, to be more accurate to our system, there are two consideration we must make. Firstly, the sample constantly loses heat, secondly, the other parts of the setup contribute to the heat capacity.

Loss of Heat of the Sample

The sample loses heat in various ways, for example, from heat conduction with the surrounding (low-pressure) air or just thermal radiation. We try to resolve these potential effects by finding out how much the initial temperature ΔT_x would have increased if there had not been exchange with the environment.

A more realistic depiction of the heating process in the experiment is shown in Figure 4. ΔT_x is found by firstly considering that it cannot depend on the heating time t_h. Therefore in an adiabatic process where $\lim t_h \to 0$ the heating line between t_2 and t_3' would be vertical, there would be no thermal exchange with the environment and we could measure ΔT_x by just measuring the length of this vertical segment. Therefore we want to find t_x where areas F_1 and F_2 are equal. The justifications behind this are:

Taking T_0 such that $T_2 < T_0 < T_3$, the exchange of heat over time is defined as the difference in temperature.

$$\frac{dQ}{dt} = k(T_0 - T)$$

Therefore, we can calculate the heat exchange difference of the ideal curve $T_i(t)$ and the actual curve $T_m(t)$ as:

$$\Delta Q_1 = Q_{1i} - Q_{1m} = k \int_{t_2}^{t_x} T_0 - T_i(t)dt - k \int_{t_2}^{t_x} T_0 - T_m(t)dt = kF_1$$

and for the second part of the process:

$$\Delta Q_2 = Q_{2f} - Q_{2m} = k \int_{t_2}^{t_x} T_f(t) - T_m(t)dt = kF_2$$

Therefore, the total error vanishes if and only if $F_1 = F_2$, justifying our claim:

$$\Delta Q = \Delta Q_1 + \Delta Q_2 = k(F_1 - F_2)$$

Corrections for Calorimeter Components

Additionally, the teflon parts and wires contribute towards the total heat capacity. This gives us the equality:

$$m_{\text{Be}} \cdot c_{\text{Be}} \cdot \Delta T_x + m_{\text{wire}} \cdot c_{\text{wire}} \cdot \Delta T_x + m_{\text{teflon}} \cdot c_{\text{teflon}} \cdot \Delta T_x = VI \cdot t_h$$

This gives us the specific heat capacity of Beryllium at constant pressure as:

$$c_{\text{Be}} = \frac{VI \cdot t_h}{\Delta T_x \cdot m_{\text{Be}}} - \frac{m_{\text{wire}}}{m_{\text{Be}}} \cdot c_{\text{wire}} - \frac{m_{\text{teflon}}}{m_{\text{Be}}} \cdot c_{\text{teflon}} \qquad (2)$$
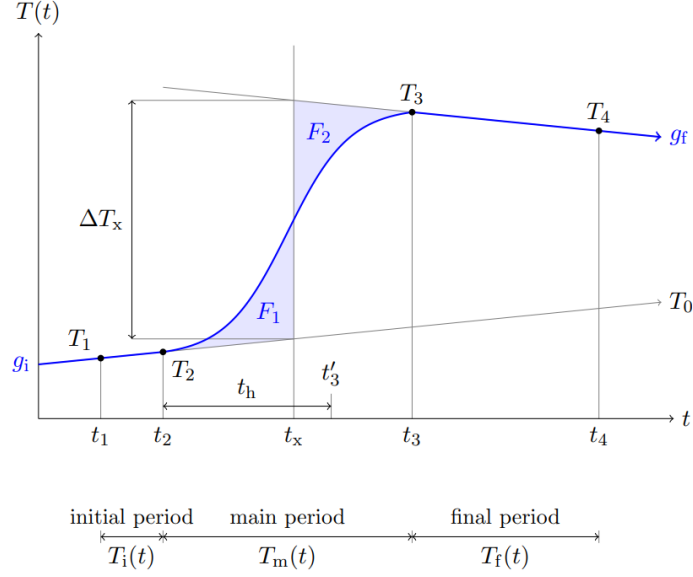
With c_P, we can find c_V with the correction 3.

Figure 4: Experimental model of the heating process

$$c_V = c_P - \frac{9\alpha^2}{\chi} \cdot \frac{M}{\rho} \cdot T \tag{3}$$

Where $M = 9.01 \cdot 10^{-3}$ is the molar mass, $\rho = 1848 \frac{kg}{m^3}$ is the density, $\alpha = 11.4 \cdot 10^{-6}$ is the linear expansion coefficient and $\chi = 7.7 \cdot 10^{-12} Pa^{-1}$ is the compressibility. [4]

Experimental Procedure

First, we create an equilibrium between the sample and the environment by an exchange gas (helium). We begin each measurement procedure by creating a vacuum. This is done by turning on the vacuum pump and slowly opening the valve between the pump and the calorimeter. Then changing the temperature in $10 - 5°C$ intervals, we make measurements of the specific heat capacity as described in the previous section. To cool our system down to a feasibly low temperature $(-190°C)$ we dip our calorimeter into liquid nitrogen.

Results

The results are summarized in Table 1 and graphically represented in Figure 5. The calculation of each heat capacity comes from the raw data packed in the appendix on Figure 6, 7, 8 and 9.

Discussion

We begin by observing Measurement 1 where we see that at higher temperatures we have extremely spread out and unpredictable data points. There is no theoretical reason for such sporadic behaviour especially considering that the melting point of beryllium is

Table 1: Measured Specific Heat Capacities for Materials M1 and M2

Measurement 1		Measurement 2	
Temperature (K)	C_p $(\mathrm{J\,kg^{-1}\,K^{-1}})$	Temperature (K)	C_p $(\mathrm{J\,kg^{-1}\,K^{-1}})$
289.15	4378	89.15	189
296.15	1272	101.65	350
302.15	4446	116.65	524
310.15	11 141	131.65	710
320.15	7149	149.15	839
330.15	3317	169.15	996
340.15	3523	189.15	1249
350.15	2043	209.15	1329
360.15	3035	229.15	1491
369.15	3060	199.15	3064
		219.15	2870
		239.15	2007

much larger than our range of observation. Despite that looking at the raw data of Figure 9, the raw data observed is quite precise and doesn't lead towards much statistical or methodical error. A possible conclusion is that all though the raw data is accurate, the calculation of the heat capacity is flawed. This seems to be the most likely cause for the poor results, but considering that the data trend doesn't stray too far away from Measurement 2's data, hints that the specific heat calculation isn't the cause for error. Additionally, since the same method and code was used for Measurement 2 where the data is much more predictable, the difficulties of Measurement 1's results probably come from poor experimental condition of the system within the temperature range 270K to 370K.

A potential improvement for Measurement 1 would be to extrapolate the behavior of the lower temperature range (Measurement 2) and compare it with recorded data points while executing the experiment. This would help finding where potential methodical errors occur. Otherwise, one can simply do multiple measurements of each temperature of interest.

Measurement 2, as already stated, has a good, almost linear behavior and was relatively close to the expected theoretical value. Since this was the second attempt at measuring, the experimenter better understands the setup and can execute the measurement with more precision. Despite this we see that at the higher temperature range of Measurement 2, outliers begin to pop up, implying instability in the results which further supports the hypothesis that the experimental setup is less reliable at higher temperature ranges. Despite the high level of predictability, in Figure 6 it's apparent that the raw data has a lot of noise. This implies that the lower temperature measurements are also quite imprecise.

In conclusion, noise, being a statistical factor, can only really be dealt with by improving the mechanics of the experimental devices. In other words, further minimize the external factors that affect the experiment. Otherwise, during the experiment, the calorimeter was not completely submerged in liquid nitrogen, meaning that at very low temperatures, we expect a fluctuation, as is seen in the data.
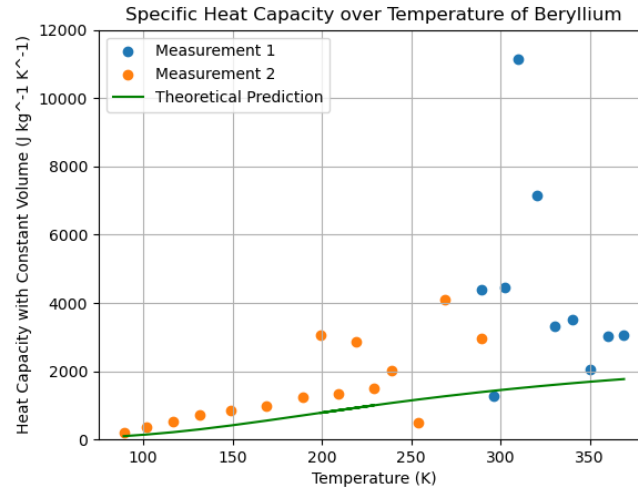
Figure 5: Experimental model of the heating process

Conclusion

Measurements 1 and 2 are relatively consistent with each other but show strong fluctuation in the higher temperature range. Looking at the collection of raw data, we see that on the other hand we expect a more reliable outcome from Measurement 1 close to our theoretical value. This opposing behaviour implies that the heat capacity can be well approximated despite noisy data, but suffers from other parameters as temperatures increase. The conclusion is that we need a more thorough and precise experimental procedure, where we compare our results to see at what point exactly strong errors appear. Otherwise we've found a decent approximation for the heat capacity of Beryllium within the range 140 K to 250 K and can potentially model how the Debye temperature changes in this range. This result is summarized in 1.

Appendix

This report benefitted from ChatGPT and DeepSeek for LaTeX table formatting and python syntax recollection. However, it was not used to write text or code.

References

[1] ETH Zurich.
    Specific Heat Capacity Measurement Manual.
    https://p3p4.phys.ethz.ch/manuals/SpecificHeat12_2014.pdf

[2] Wikipedia.
    Heat Capacity.
    https://en.wikipedia.org/wiki/Heat_capacity

[3] Wikipedia.
    Equipartition Theorem.
    https://en.wikipedia.org/wiki/Equipartition_theorem

[4] Wikipedia.
Beryllium.
https://en.wikipedia.org/wiki/Beryllium
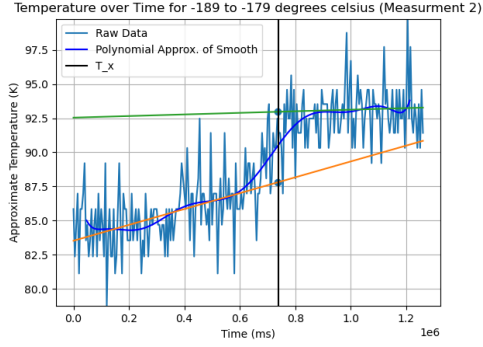
(a) -189 °C to -179 °C
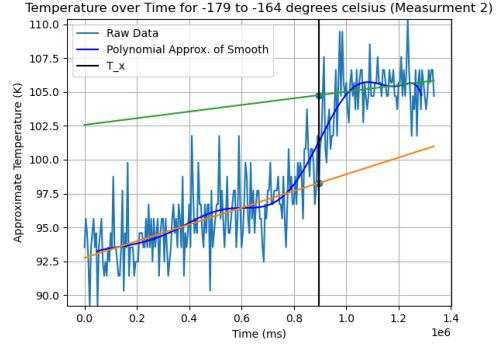
(b) -179 °C to -164 °C
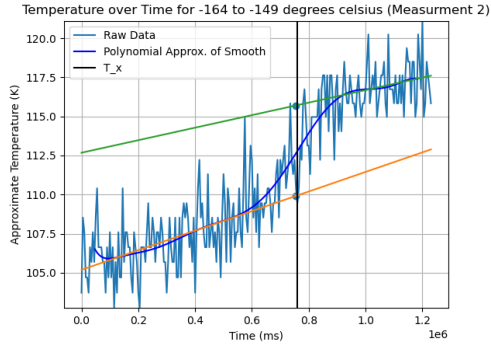
(c) -164 °C to -149 °C
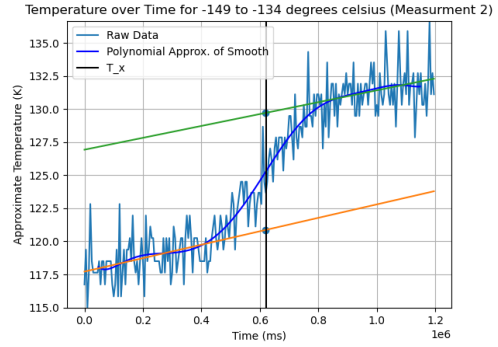
(d) -149 °C to -134 °C
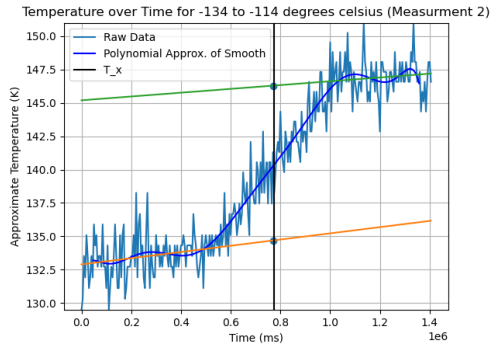
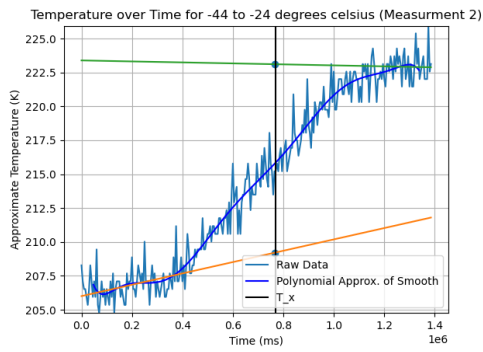(e) -134 °C to -114 °C
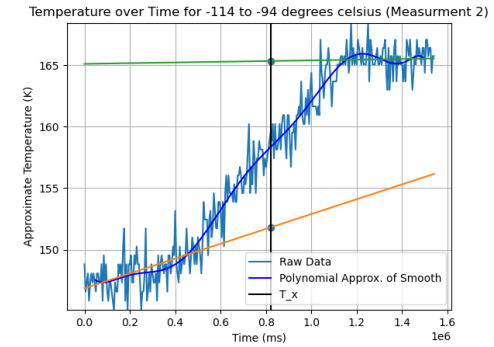
(f) -114 °C to -94 °C

Figure 6: Raw Data and fits for approximating the resulting heat capacity of Beryllium
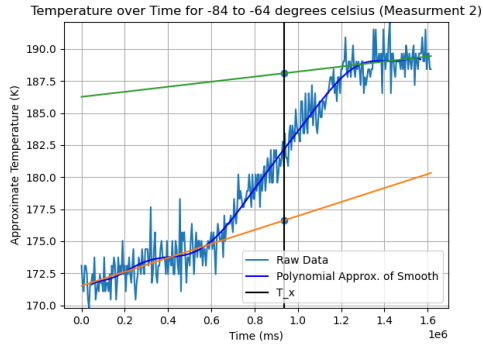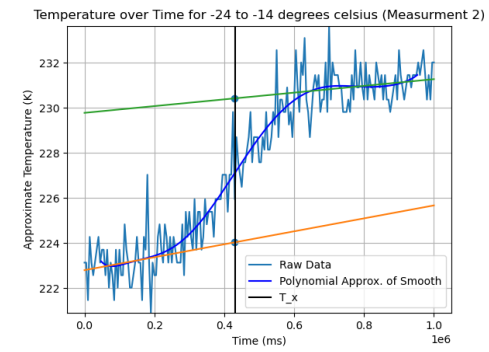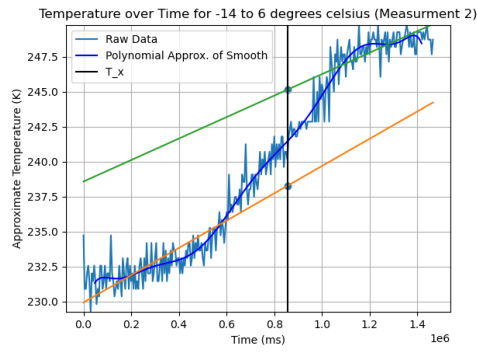
(a) -84 °C to -64 °C
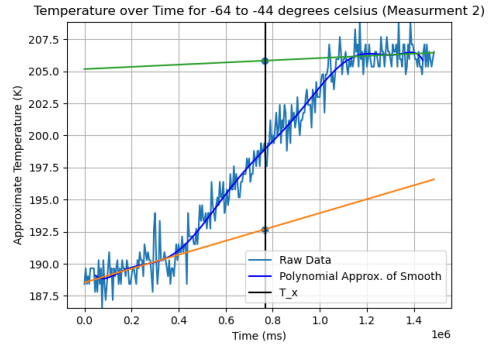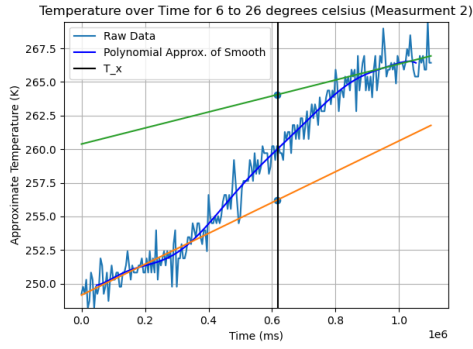
(b) -64 °C to -44 °C

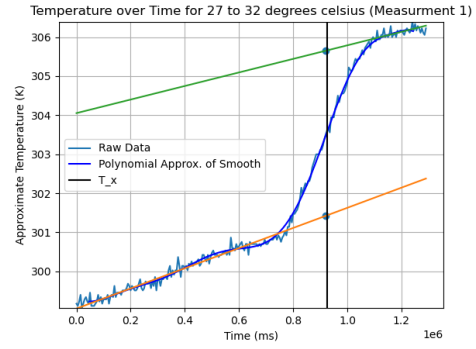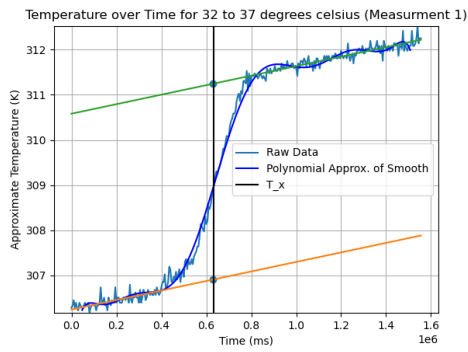(c) -44 °C to -24 °C
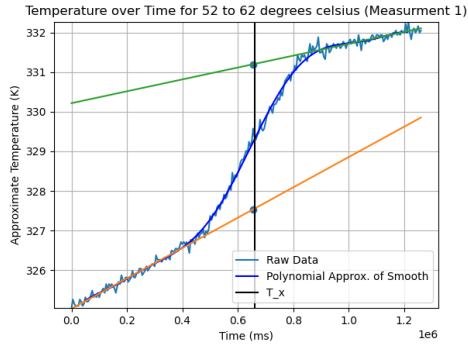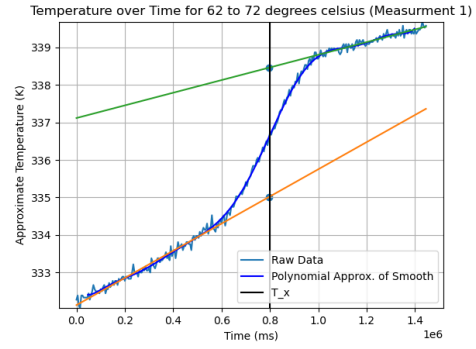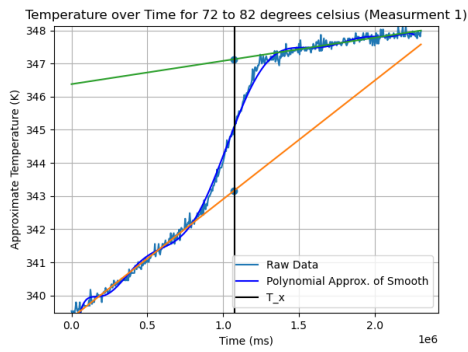
(d) -24 °C to -14 °C

(e) -14 °C to 6 °C

Figure 7: Raw Data and fits for approximating the resulting heat capacity of Beryllium Part 2

(a) $6\,^{\circ}\mathrm{C}$ to $26\,^{\circ}\mathrm{C}$

(b) $27\,^{\circ}\mathrm{C}$ to $32\,^{\circ}\mathrm{C}$

(c) $32\,^{\circ}\mathrm{C}$ to $37\,^{\circ}\mathrm{C}$
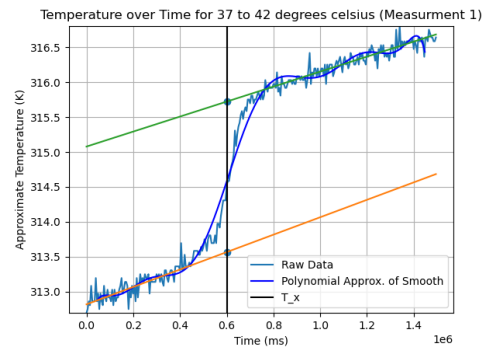
(d) $37\,^{\circ}\mathrm{C}$ to $42\,^{\circ}\mathrm{C}$
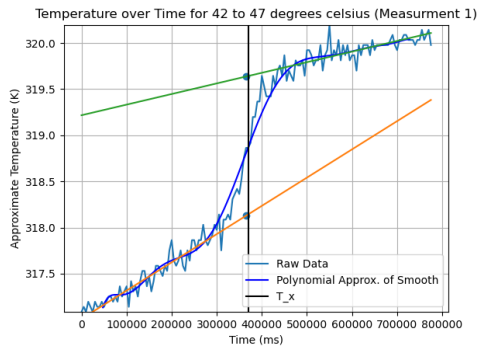
(e) $42\,^{\circ}\mathrm{C}$ to $47\,^{\circ}\mathrm{C}$
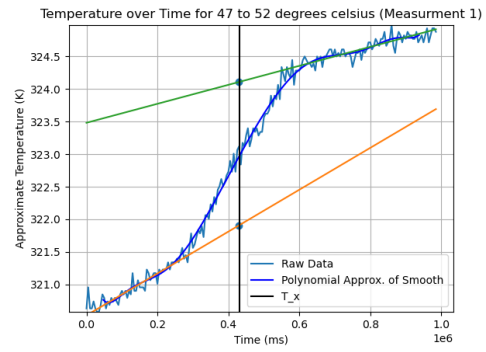
(f) $47\,^{\circ}\mathrm{C}$ to $52\,^{\circ}\mathrm{C}$

Figure 8: Raw Data and fits for approximating the resulting heat capacity of Beryllium Part 3
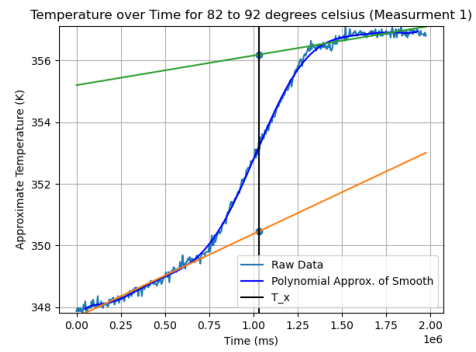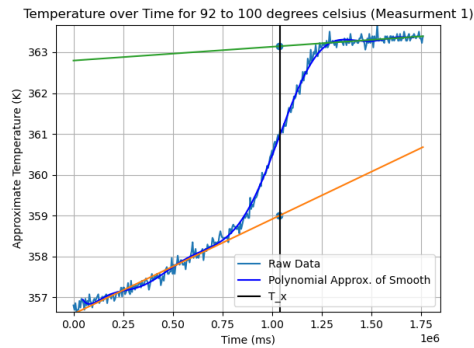
(a) 52 °C to 62 °C

(b) 62 °C to 72 °C

(c) 72 °C to 82 °C

(d) 82 °C to 92 °C

(e) 92 °C to 100 °C

Figure 9: Raw Data and fits for approximating the resulting heat capacity of Beryllium Part 4